Organic & Biomolecular Chemistry

PAPER

View Article Online
View Journal | View Issue

Cite this: *Org. Biomol. Chem.*, 2019, **17**, 7956

Three-state switching in a double-pole change-over nanoswitch controlled by redox-dependent self-sorting†

Sudhakar Gaikwad, Merve Sinem Özer, Susnata Pramanik and Michael Schmittel *

Received 28th June 2019,
Accepted 7th August 2019

DOI: 10.1039/c9ob01456j

rsc.li/obc

The four-arm nanomechanical switch **1** with four different terminals exhibits two switching arms (contacts A and D) and two distinct stations for binding (contacts B and C). In switching State I, the azaterpyridine arm is intramolecularly coordinated to a zinc(II) porphyrin station (connection A ↔ B) while contact D (a ferrocenylbipyridine unit) and contact C (phenanthroline) remain disconnected. After addition of copper(I) ions (State II) both connections A ↔ B and C ↔ D are established. Upon one-electron oxidation, double-pole change-over switching cleaves both connections A ↔ B & C ↔ D and establishes the new connection A ↔ C (State III). Fully reversible three-state switching (State I → State II → State III → State II → State I) was achieved by adding appropriate chemical and redox stimuli.

Introduction

In the quest for technological applications, a good variety of molecular switches have been reported that undergo nanomechanical toggling upon addition and/or removal of electrons.[1,2] Despite spectacular cases of two-state switches,[1,2] examples of multi-state toggling (three and more states) including at least one redox-driven switching event remain scarce.[3] Actually, full reversibility in molecular switches with three and more states remains a general challenge toward the development of multifunctional devices.[4]

Further challenges encompass the development of switching protocols that involve entangled nanomechanical motions, for instance when a toggling arm is replaced by another arm in a single step giving rise to a double-pole change-over switching. Such an entangled switching event is valuable because electronic and steric changes effectively happen at four sites simultaneously and may ignite a number of follow-up processes. Herein, we would like to report on a case of double-pole change-over switching by presenting nanoswitch **1** and its three-state toggling. In the key switching step, it involves self-sorting[5] triggered by oxidation/reduction of a ferrocene-appended bipyridine ligand. Reliable redox-state dependent self-sorting has been demonstrated earlier in rotors,[1a] in a two-state nanoswitch,[2d] in chemical communication between up to three nanoswitches,[6] and in switchable catalysis.[2k]

To accomplish three-state switching using chemical and electrochemical stimuli, we chose to integrate two distinct switching arms and stations into switch **1**. As a result, four different terminals are attached at the central tetraphenylmethane core of **1**, *i.e.* a (i) sterically shielded diarylphenanthroline ($phenAr_2$) station, (ii) zinc(II) porphyrin (ZnPor) station, (iii) ferrocene-appended bipyridine (fcbipy) arm, and (iv) an azaterpyridine (azatpy) arm. For three-state switching altogether three orthogonal coordination binding motifs are needed, which are the (i) HETPHEN[7] (HETeroleptic PHENanthroline) complexation in presence of copper(I) ions, (ii) HETTAP[8] (HETeroleptic Terpyridine And Phenanthroline) complexation after oxidation and (iii) N_{azatpy} → ZnPor interaction.[9]

In State I (= nanoswitch **1**) the azatpy arm is intramolecularly locked at the ZnPor station. After addition of copper(I) ions, we would expect that the presence of the fcbipy arm with its electron-rich ferrocene-appended bipyridine in **1** leads to the selective formation of the intramolecular HETPHEN-type[7] complex $[Cu(fcbipy)(phenAr_2)]^+$ which should be favored over the HETTAP complex[8] $[Cu(azatpy)(phenAr_2)]^+$. This binding preference in $[Cu(\mathbf{1})]^+$ (State II) is warranted due to (i) a stronger binding of the electron-rich fcbipy unit to the copper(I)-loaded phenanthroline and (ii) the additional stabilization gained from maintaining the N_{azatpy} → ZnPor interaction. Upon oxidation at ferrocene, the binding strength of the fcbipy unit should be sufficiently reduced to allow toggling of the azatpy rotary arm in $[Cu(\mathbf{1})]^{2+}$ from the ZnPor station to the copper(I) phenanthroline site thus affording a HETTAP

Center of Micro-and Nanochemistry and Engineering, Organische Chemie I, Universität Siegen Adolf-Reichwein-Strasse-2, 57068 Siegen, Germany.
E-mail: schmittel@chemie.uni-siegen.de

†Electronic supplementary information (ESI) available. See DOI: 10.1039/c9ob01456j

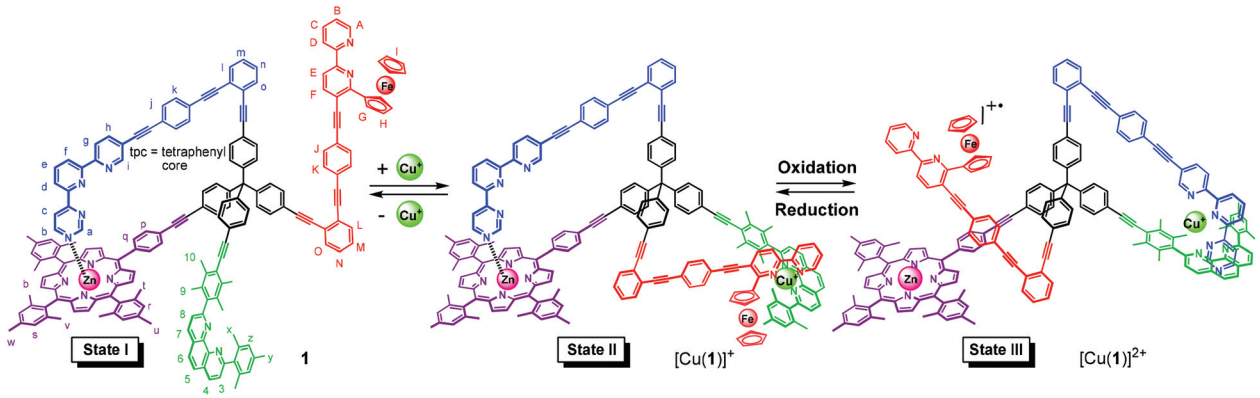

Fig. 1 Three-state switching in nanoswitch **1**.

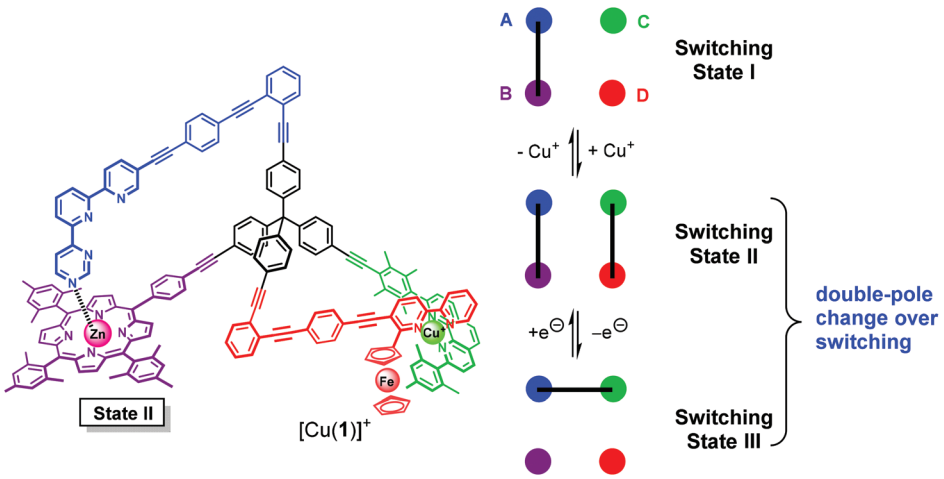

Fig. 2 Nanoswitch **1** and the connections in all switching states.

complex (State III). Upon reduction of the ferrocenium unit, the binding strength of the fcbipy unit should be restored to regenerate State II. Finally, removal of copper(I) ions with 2-ferrocenyl-9-mesityl-[1,10]-phenanthroline is expected to reset the original locked State I (Fig. 1). Interconversion of States II and III fulfills the criteria for a double-pole change-over switching process (Fig. 2).

Results and discussion

Synthesis

Nanoswitch **1** was prepared through a series of Sonogashira cross-coupling reactions as shown in Scheme 1. First, 6-ferrocenyl-5-((trimethylsilyl)ethynyl)-2,2′-bipyridine[10] (**2**) was deprotected in aq. K_2CO_3, THF and methanol yielding compound **3** in 74% yield. The Sonogashira reaction of compound **3** with ((4-bromophenyl)ethynyl)trimethylsilane[11] in a mixture of THF/triethylamine in presence of $Pd(PPh_3)_4$ as a catalyst furnished compound **4** in good yield. Compound **4** was converted to the terminal ethynyl derivative **5** by treatment with aq. K_2CO_3 in THF and methanol. A follow-up Sonogashira coupling of compound **5** with 1,2-diiodobenzene using Pd(0) catalyst in anhydrous DMF and triethylamine provided the rotary arm **6** in 63% yield. Finally, Sonogashira coupling of compound **6** with the known scaffold **7** [4c] using Pd(0) as catalyst in anhydrous DMF and triethylamine furnished nanoswitch **1** in 22% yield.

Nanoswitch **1** was fully characterized using NMR, UV-vis spectroscopy, ESI-MS, and elemental analysis. The ESI-MS displays a molecular ion peak at m/z = 1309.7 that is diagnostic for the doubly protonated $[\mathbf{1}\cdot 2H]^{2+}$ with the experimental isotopic splitting pattern matching the computed one (ESI, Fig. S32†). In the ^{1}H NMR spectrum of **1**, pyrimidine protons a-H and b-H of the azatpy arm are located in the aliphatic region at 3.76 and 2.73 ppm, respectively, which confirms the immersion of the terminal pyrimidine (pym) ring into the ZnPor's shielding zone suggesting a $N_{azatpy} \rightarrow$ ZnPor interaction (ESI, Fig. S13†). The sharp signals of protons a-H and b-H are concentration independent (c = 0.55 mM to 2.9 mM, in CD_2Cl_2, ESI, Fig. S17†) precluding intermolecular coordination. Equally, the Q-band absorption of **1** at 561 nm

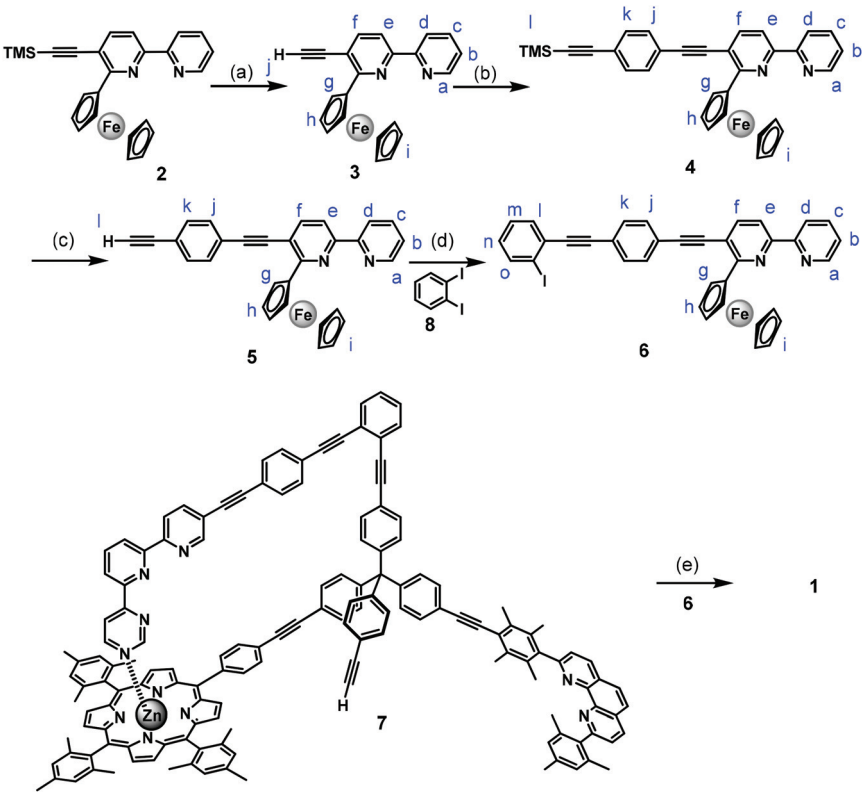

Scheme 1 Synthesis of nanoswitch **1**. (a) aq. K_2CO_3, MeOH–THF, 74%; (b) $Pd(PPh_3)_4$, THF–Et_3N, 60 °C, 18 h, 98%; (c) aq. K_2CO_3, MeOH–THF, 98%; (d) $Pd(PPh_3)_4$, THF–Et_3N, 60 °C, 18 h, 63%; (e) $Pd(PPh_3)_4$, DMF–Et_3N, 60 °C, 24 h, 22%.

remained constant when the concentration was varied from c = 10^{-6} to 10^{-4} M (in DCM, ESI, Fig. S24†). Moreover, the Soret band absorption of **1** at 429 nm ($c = 10^{-6}$ M, in DCM) supports the coordination of the pyrimidine ^{4}N nitrogen to the ZnPor station. The 8 nm bathochromic shift of the Soret band in **1** may be compared to that of an uncoordinated tetraphenyl zinc porphyrin (ZnTPP) at 421 nm (ESI, Fig. S23†).[9,12] In summary, combined ^{1}H NMR and UV-vis data corroborate intramolecular coordination of the pyrimidine ring to the zinc porphyrin unit in **1**.

Three-state switching in nanoswitch 1

At first, we investigated reversible switching between States I and II by addition and removal of copper(I) ions. Addition of 1.0 equiv. of $[Cu(CH_3CN)_4][B(C_6F_5)_4]$ to a solution of **1** in dichloromethane-d_2 resulted in the formation of the intramolecular HETPHEN complex $[Cu(\mathbf{1})]^+$ (= State II) in 96% yield. The assignment was corroborated by ^{1}H, ^{1}H–^{1}H COSY, ESI-MS and UV-vis data. The ^{1}H NMR was informative in various ways: signals of phenanthroline protons z-H at δ = 6.95 ppm shifted and split into four sets at δ = 6.97, 6.72 and 6.96, 6.70 ppm as a result of breaking the local symmetry and formation of two diastereomers in 55 : 45 ratio. In addition, bipyridine protons A-H and E-H were upfield shifted from δ = 8.57 and 8.22 ppm to δ = 7.56 and 7.77 ppm, respectively, due to ring currents of the phenanthroline aryl groups (Fig. 3B). These NMR observations thus unambiguously confirmed formation of $[Cu(\mathbf{1})]^+$ (= State II). The ESI-MS analysis of the resultant complex exhibited a molecular ion peak at m/z = 2741.1 (*i.e.* $[Cu(\mathbf{1})\cdot MeCN\cdot H_2O]^+$) supporting formation of State II (ESI, Fig. S33†). The complexation constant of $[Cu(\mathbf{1})]^+$ was determined using a UV-vis titration as log K = 9.39 (ESI, Fig. S42†).

In addition, a UV-vis study of $[Cu(\mathbf{1})]^+$ showing the Q-band absorption at 561 nm proved the existence of $N_{azatpy} \rightarrow$ ZnPor coordination in State II (ESI, Fig. S25†). Addition of 2.0 equiv. of 2-ferrocenyl-9-mesityl-[1,10]-phenanthroline regenerated **1**, *i.e.* the original locked State I. Reversible switching between States I and II was checked for two cycles by addition and removal of copper(I) ions (ESI, Fig. S20†).

Thereafter, we investigated reversible switching between States II and III by redox input. A combined cyclic voltammetry (CV) and differential pulse voltammetry (DPV) study of $[Cu(\mathbf{1})]^+$ in dichloromethane displayed $E_{1/2}$ = 0.74 and 0.78 V_{SCE} for Fc/Fc^+ and ZnPor$^{0/+}$ transitions (Fig. S38 & 39†). In contrast, with 1 vol% of acetonitrile, the complex $[Cu(\mathbf{1})]^+$ revealed two well separated oxidation steps (Fig. 4), *i.e.* Fc/Fc^+ at $E_{1/2}$ = 0.47 V_{SCE} and ZnPor$^{0/+}$ at $E_{1/2}$ = 0.67 V_{SCE}, while the third wave at $E_{1/2}$ = 1.11 V_{SCE} is attributed to the $Cu^{+/2+}$ transition. The data of **1** with $E_{1/2}$ = 0.45 V_{SCE} for Fc/Fc^+ and ZnPor$^{0/+}$ at $E_{1/2}$ = 0.66 V_{SCE} as a reference (Fig. S36 & S37†) suggest that in acetonitrile the ferrocenyl arm upon oxidation readily detaches from the copper(I) site.

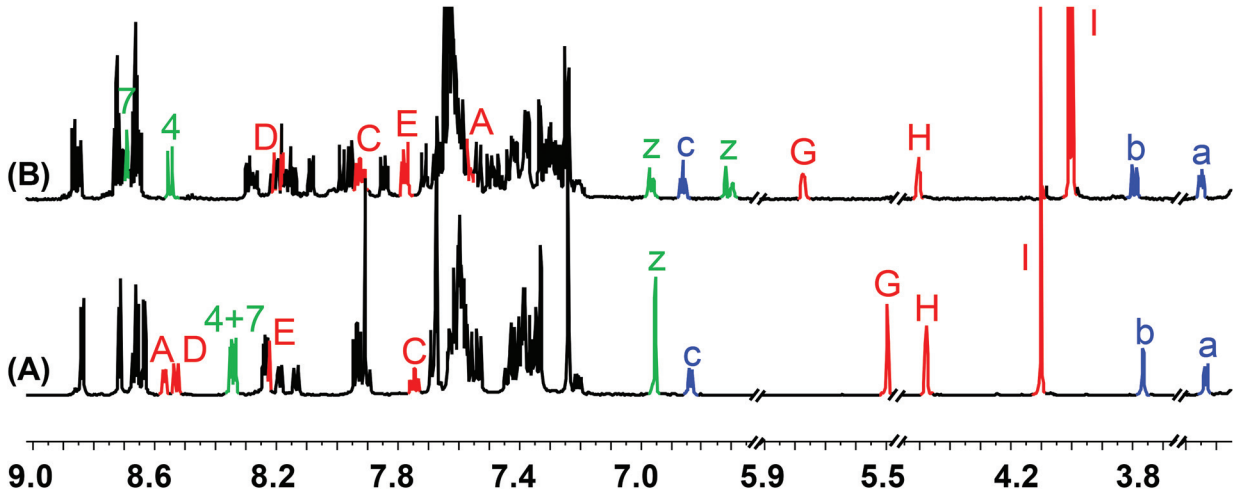

Fig. 3 Comparison of partial ^{1}H NMR spectra (600 MHz, CD_2Cl_2, 298 K) of (A) nanoswitch **1** = Switching State I and (B) complex $[Cu(\mathbf{1})]^{+}$ = Switching State II.

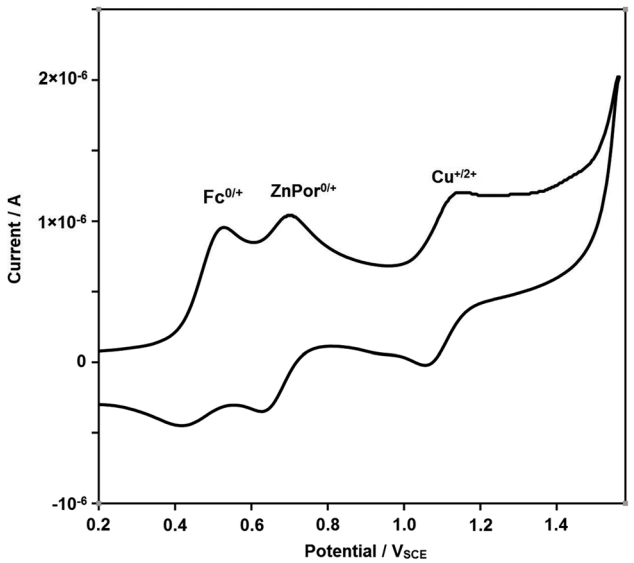

Fig. 4 CV of complex $[Cu(\mathbf{1})]^{+}$ (scan rate of 100 mV s^{-1}) in dichloromethane + 1 vol% dry acetonitrile: $Fc^{0/+}$ at $E_{1/2}$ = 0.47 V_{SCE}, $ZnPor^{0/+}$ at $E_{1/2}$ = 0.67 V_{SCE} and $Cu^{+/2+}$ at $E_{1/2}$ = 1.11 V_{SCE}.

Even at a low scan rate of 50 mV s^{-1} and in presence of 1 vol% of acetonitrile for accelerating metal–ligand dissociation, the CV (ESI, Fig. 4†) did not show any indication of redox toggling of the azatpy rotary arm. Because switching of the azatpy arm could not be detected due to the inadequate timescale of CV, we decided to utilize chemical redox reagents.[13] For chemical oxidation, we used tris(4-bromophenyl)aminium hexachloroantimonate ($TBA^{+\bullet}SbCl_6^{-}$) or tris(4-bromophenyl)aminium tetrafluoroborate ($TBA^{+\bullet}BF_4^{-}$), and for reduction[13] decamethylferrocene (dmfc) or 3-(11-bromoundecyl)-1,1′-biferrocenylene (BFD).[14]

At first, 1.0 equiv. of $TBA^{+\bullet}SbCl_6^{-}$ was added to a solution of $[Cu(\mathbf{1})]^{+}$ in dichloromethane, then after 5 min an oxidative scan was started that showed a new oxidation peak at 0.69 V_{SCE} (ESI, Fig. S40†) which indicated the presence of a copper HETTAP complex and thus formation of State III (= $[Cu(\mathbf{1})]^{2+}$). Then the resultant solution of State III was treated with 1.0 equiv. of dmfc. Two min after mixing a scan showed the CV signature of State II, *i.e.* oxidation waves at 0.59 V_{SCE} (merged wave for $Fc^{0/+}$ and $ZnPor^{0/+}$) and at 1.16 V_{SCE} (for Cu^{+}/Cu^{2+}) (see ESI, Fig. S41†). Apparently, the reduction of the ferrocenium unit in $[Cu(\mathbf{1})]^{2+}$ regenerated the electron-donating fcbipy unit thus triggering formation of the HETPHEN complex of the fcbipy unit with the copper(I)-phenanthroline station. At the same time the azatpy arm returned to the ZnPor station.

The equilibrium position in State III was assessed by a thermochemical cycle (ESI, Fig. S43†) based on $\log K$ = 9.39 determined for $[Cu(\mathbf{1})]^{+}$ (ESI, Fig. S42†). In dichloromethane, the change of the ferrocene potential in the metal-free nanoswitch **1** ($Fc^{0/+}$, $E_{1/2}$ = 450 mV_{SCE}) and in its Cu^{+} complex ($Fc^{0/+}$, $E_{1/2}$ = 740 mV_{SCE}, ESI, Fig. S39†) show a reduced binding in the $[Cu(fcbipy^{+\bullet})(phenAr_2)]^{+}$ complex of $\log K$ = 4.5 (ESI, Fig. S43†).[6b] In contrast, the $[Cu(azatpy)(phenAr_2)]^{+}$ complex in State III is known from earlier work on $[Cu(\mathbf{7})]^{+}$ to correspond to $\log K$ = 7.42, a rather low value for a HETTAP complex since it incorporates the parallel cleavage of the N → ZnPor interaction. Switching the azatpy arm in the process of State II → III thus involves a stronger binding of the $[Cu(azatpy)(phenAr_2)]^{+}$ unit by $\Delta\log K$ = 7.4–4.5 = 2.9. This data suggests a 99.9% preference of the $[Cu(azatpy)(phenAr_2)]^{+}$ over the $[Cu(fcbipy^{+\bullet})(phenAr_2)]^{+}$ complexation site in State III (ESI, Fig. S44†).

Switching between States II and III was extensively studied by UV-vis and ESI-MS spectroscopy. When 1.0 equiv. of $TBA^{+\bullet}SbCl_6^{-}$ was added to a solution of $[Cu(\mathbf{1})]^{+}$ in dichloromethane (c = 2 × 10^{-4} M), the Q-band absorption at 561 nm shifted to 553 nm within 12 min at room temperature (Fig. 5, blue trace and ESI, Fig. S27†). This 8 nm shift is in perfect agreement with a swing of the azatpy rotary arm from the ZnPor station to the copper(I)-phenanthroline binding site and concomitant formation of the HETTAP complex. After oxi-

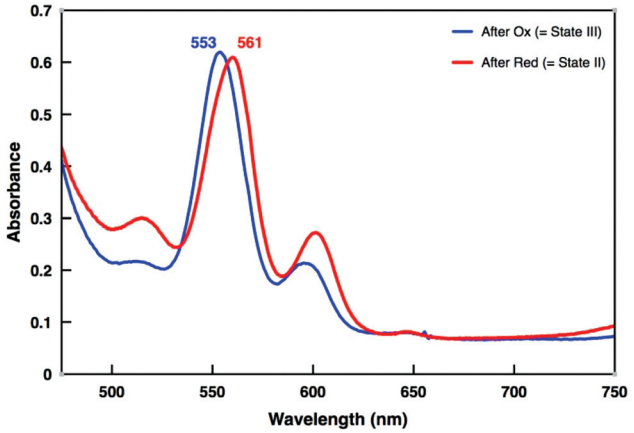

Fig. 5 UV-vis spectra: Blue trace: Oxidation of State II by $TBA^{+\bullet}SbCl_6^-$ furnishes State III (Fig. 1). Red trace: Reduction of State III by dmfc generates State II.

dation the ESI-MS spectrum displayed a molecular ion peak at m/z = 1340.9 Da that corresponds to $[Cu(\mathbf{1})]^{2+}$ with the experimental isotopic splitting pattern matching with the calculated one (Fig. S34†). State III was then treated with one equiv. of dmfc as reducing agent. The Q-band of the resultant solution fully shifted from 553 to 561 nm within 1 min at room temperature suggesting intramolecular return of the azatpy arm to the ZnPor station (Fig. 5, red trace and ESI, Fig. S27†). The ESI-MS spectrum of the resultant solution shows a molecular ion peak at m/z = 2738.4 Da for $[Cu(\mathbf{1})\cdot CH_3CN\cdot H_2O]^+$ that is assigned to State II (ESI, Fig. S35†).

The switching process from State III → II was also studied by ^{1}H NMR now using 3-(11-bromoundecyl)-1,1′-biferrocenylene (BFD) as a reducing agent because its oxidation produces a diamagnetic species. Hereunto, the solution of State II was first oxidized by addition of one equiv. of $TBA^{+\bullet}BF_4^-$. Subsequent treatment with BFD provided $[Cu(\mathbf{1})]^+$ in 95 : 5 selectivity of $[Cu(fcbipy)(phenAr_2)]^+$: $[Cu(azatpy)(phenAr_2)]^+$ (ESI, Fig. S21†), slightly different from the thermodynamically expected 99 : 1 ratio derived from the known log K values.

Next we examined the switching between all three states by addition of appropriate chemical inputs: State I → State II → State III → State II → State I. Addition of 1.0 equiv. of $[Cu(CH_3CN)_4][B(C_6F_5)_4]$ to a solution of **1** (State I) in dichloromethane-d_2 provided the HETTAP complex $[Cu(\mathbf{1})]^+$ (= State II). The complex $[Cu(\mathbf{1})]^+$ was then treated with 1.0 equiv. of $TBA^{+\bullet}BF_4^-$ to afford $[Cu(\mathbf{1})]^{2+}$ (= State III) which was subsequently reduced by addition of 3-(11-bromoundecyl)-1,1′-biferrocenylene to afford State II in 94% yield. Finally, 2.0 equiv. of 2-ferrocenyl-9-mesityl-[1,10]-phenanthroline was added to reset to the original locked State I (ESI, Fig. S22†).

The reversible double-pole change-over switching process as demonstrated in State II → State III → State II is readily understood since the binding strength of the fcbipy arm is notably deteriorated by oxidation of the ferrocenyl unit by $\Delta\log K$ = 4.9 (*vide supra*). As a result, the azatpy arm detaches from the ZnPor site and associates with the copper(I) phenanthroline site.

Conclusion

We describe the synthesis of the nanomechanical switch **1** in which four distinct terminals are mounted on a tetraphenylmethane scaffold. Bidirectional switching of nanoswitch **1** between three different states is revealed upon addition of chemical and redox inputs. A key step is the reversible double-pole change-over switching process that was ignited by one-electron oxidation and reduction of the ferrocenyl subunit and that involves electronic and steric changes at all four terminals. In detail, upon oxidation/reduction two toggling arms, an azaterpyridine and a ferrocenylbipyridine arm, dissociate from their binding sites and reversibly exchange at the copper(I) phenanthroline station.

Experimental

General information

All reagents were obtained from commercial providers and used without further purification. Technical grade solvents were distilled prior to use. Tetrahydrofuran (THF) was predried over basic alumina and then distilled over potassium. Dimethylformamide (DMF) and triethylamine were distilled on calcium hydride. Melting points of compounds were measured using a Büchi SMP-11 instrument. ^{1}H, ^{13}C, and ^{1}H–^{1}H COSY NMR spectra were recorded on Bruker Avance 400 and Varian (600 MHz) spectrometers. Chemical shifts refer to the residual protiated fraction of the NMR solvent ($CHCl_3$: δ_H = 7.26 ppm, δ_C = 77.0 ppm; $CHDCl_2$: δ_H = 5.32 ppm, δ_C = 53.8 ppm). Abbreviations were used in ^{1}H NMR assignments to describe splitting patterns (s: singlet, d: doublet, t: triplet, dd: doublet of doublet, ddd: doublet of doublet of doublet, bs: broad singlet, td: triplet of doublets, quint: quintet, m: multiplet), the value of coupling constant(s) is reported in Hertz (Hz) and the number of protons are implied. Numbering of the carbon atoms is not in accordance with IUPAC nomenclature. UV-vis spectra were measured on a Cary Win 50 spectrometer. Electrospray ionization mass spectra (ESI-MS) were recorded on a Thermo-Quest LCQ Deca instrument. Infrared (IR) spectra were recorded using a PerkinElmer Spectrum-Two FT-IR spectrometer. Column chromatography was performed on silica gel 60 (60–230 mesh) or on neutral alumina (0.05–0.15 mm, Brockmann Activity 1). Thin layer chromatography (TLC) was performed using Merck silica gel (60 F254) or on neutral Al_2O_3 (150 F254) sheets. Size exclusion chromatography was performed on BioRads Biobeads-SX3 using toluene or tetrahydrofuran as an eluents.

The cyclic voltammetry (CV) and DPV experiments were carried out by using a standard three-electrode setup (1.0 mm Pt working electrode, Pt auxiliary electrode, and a silver wire as the reference electrode) connected to a Princeton Applied Research PARSTAT 2273 Advanced Electrochemical System. Calibration was done with 2,4,6-triphenylpyrylium tetrafluoroborate ($E_{1/2}$ = −0.39 V *vs.* SCE) or dmfc as an internal standard ($E_{1/2}$ = −0.14 V *vs.* SCE).

5-Ethynyl-6-ferrocenyl-2,2′-bipyridine (3). 6-Ferrocenyl-5-((trimethylsilyl)ethynyl)-2,2′-bipyridine (**2**, 500 mg, 1.14 mmol) was dissolved in a solution THF (20 mL) and MeOH (10 mL). Thereafter, aq. K_2CO_3 (317 mg, 2.29 mmol in 10 mL of deionized H_2O) was added and the reaction mixture was allowed stirring at room temperature for 3 h. The solvent was evaporated under reduced pressure and the product was extracted in DCM (25 mL). After washing the organic layer with deionized water (50 mL), the former was dried over anhydrous $MgSO_4$. Evaporation of the solvent afforded compound **3** as an orange solid (305 mg, 0.84 mmol, 74%). **Mp**: 126–127 °C. **IR (KBr)**: $\tilde{\nu}$ = 3272, 3013, 2241, 1710, 1586, 1574, 1544, 1474, 1436, 1391, 1361, 1230, 1103, 1094, 1077, 991, 856, 831, 818, 798, 748, 721, 670, 616, 516 cm^{-1}. **^{1}H NMR ($CDCl_3$, 400 MHz)**: δ = 8.69 (ddd, ^3J = 4.8 Hz, ^4J = 1.8 Hz, ^5J = 0.9 Hz, 1H, a-H), 8.57 (ddd, ^3J = 7.6 Hz, ^4J = 1.2 Hz, ^5J = 0.9 Hz, 1H, d-H), 8.21 (d, ^3J = 8.1 Hz, 1H, f-H), 7.88 (d, ^3J = 8.1 Hz, 1H, e-H), 7.86 (td, ^3J = 7.6 Hz, ^4J = 1.8 Hz, 1H, c-H), 7.32 (ddd, ^3J = 7.6 Hz, ^3J = 4.8 Hz, ^4J = 1.2 Hz, 1H, b-H), 5.49 (t, ^3J = 2.0 Hz, 2H, g-H), 4.44 (t, ^3J = 2.0 Hz, 2H, h-H), 4.11 (s, 5H, i-H), 3.60 (s, 1H, j-H). **^{13}C NMR ($CDCl_3$, 100 MHz)**: δ = 159.3, 155.8, 154.4, 149.1, 143.2, 136.8, 123.9, 121.5, 116.7, 114.7, 84.4, 83.5, 82.9, 69.8, 69.7 (2C). **Elemental analysis**: Calcd for $C_{22}H_{16}FeN_2$: C, 72.55; H, 4.43; N, 7.69; found: C, 72.22; H, 4.41; N, 7.45. **ESI-MS**: Calcd for $[C_{22}H_{16}FeN_2{\cdot}H]^+$ = $[\mathbf{3}{\cdot}H]^+$, m/z = 365.1; found: $[\mathbf{3}{\cdot}H]^+$, m/z = 365.2.

6-Ferrocenyl-5-((4-((trimethylsilyl)ethynyl)phenyl)ethynyl)-2,2′-bipyridine (4). 5-Ethynyl-6-ferrocenyl-2,2′-bipyridine (**3**, 450 mg, 1.24 mmol) and ((4-bromophenyl)ethynyl)trimethylsilane (626 mg, 2.47 mmol) were dissolved in a mixture of anhydrous THF (25 mL) and anhydrous Et_3N (25 mL). The solution was degassed using freeze–pump–thaw procedures (3×), then $Pd(PPh_3)_4$ (143 mg, 124 μmol) was added under N_2 atmosphere. The mixture was heated to 60 °C for 18 h (TLC control) and evaporated. The residue was subjected to column chromatographic purification on silica gel (ϕ = 3.5 cm, l = 30 cm) using 5% EtOAc in *n*-hexane to furnish compound **4** as an orange solid (656 mg, 1.22 mmol, 98%). **Mp**: 183–185 °C. **IR (KBr)**: $\tilde{\nu}$ = 2999, 2952, 2209, 2150, 1585, 1571, 1541, 1502, 1473, 1431, 1386, 1247, 1218, 1105, 1030, 1001, 861, 814, 772, 740 cm^{-1}. **^{1}H NMR ($CDCl_3$, 400 MHz)**: δ = 8.70 (ddd, ^3J = 4.7 Hz, ^4J = 1.8 Hz, ^5J = 0.9 Hz, 1H, a-H), 8.59 (ddd, ^3J = 7.6 Hz, ^4J = 1.2 Hz, ^5J = 0.9 Hz, 1H, d-H), 8.25 (d, ^3J = 8.1 Hz, 1H, f-H), 7.91 (d, ^3J = 8.1 Hz, 1H, e-H), 7.86 (td, ^3J = 7.6 Hz, ^4J = 1.8 Hz, 1H, c-H), 7.57 (d, ^3J = 8.8 Hz, 2H, j-H), 7.51 (d, ^3J = 8.8 Hz, 2H, k-H), 7.33 (ddd, ^3J = 7.6 Hz, ^3J = 4.7 Hz, ^4J = 1.2 Hz, 1H, b-H), 5.50 (t, ^3J = 1.9 Hz, 2H, g-H), 4.47 (t, ^3J = 1.9 Hz, 2H, h-H), 4.11 (s, 5H, i-H), 0.28 (s, 9H, l-H). **^{13}C NMR ($CDCl_3$, 100 MHz)**: δ = 158.8, 155.8, 154.1, 149.1, 142.2, 136.8, 132.2, 131.0, 123.8, 123.3 (2C), 121.4, 116.8, 115.7, 104.5, 96.7, 95.6, 90.8, 83.7, 69.9, 69.7, 69.6, −0.1. **Elemental analysis**: Calcd for $C_{33}H_{28}FeN_2Si$: C, 73.87; H, 5.26; N, 5.22; found: C, 73.50; H, 5.21; N, 5.17. **ESI-MS**: Calcd for $[C_{33}H_{28}FeN_2Si{\cdot}H]^+$ = $[\mathbf{4}{\cdot}H]^+$, m/z = 537.1; found: $[\mathbf{4}{\cdot}H]^+$, m/z = 537.2.

5-((4-Ethynylphenyl)ethynyl)-6-ferrocenyl-2,2′-bipyridine (5). 6-Ferrocenyl-5-((4-((trimethylsilyl)ethynyl)phenyl)ethynyl)-2,2′-bipyridine (**4**, 400 mg, 746 μmol) was dissolved in a solution of THF (10 mL) and MeOH (10 mL). Then, an aqueous solution of K_2CO_3 (206 mg, 1.49 mmol in 10 mL of deionized H_2O) was added and the mixture was stirred at room temperature for 3 h. The solvent was evaporated, water (30 mL) was added, and the product was extracted in DCM (35 mL). The organic phase was removed and dried over anhydrous $MgSO_4$. After evaporation of the solvent, compound **5** was afforded as an orange solid (341 mg, 734 μmol, 98%). **Mp**: 142–144 °C. **IR (KBr)**: $\tilde{\nu}$ = 3279, 3073, 2921, 2852, 2336, 1586, 1542, 1508, 1477, 1441, 1430, 1383, 1361, 1242, 1103, 1075, 1034, 993, 837, 824, 772, 741, 663, 621, 492 cm^{-1}. **^{1}H NMR ($CDCl_3$, 400 MHz)**: δ = 8.70 (ddd, ^3J = 4.8 Hz, ^4J = 1.9 Hz, ^5J = 0.9 Hz, 1H, a-H), 8.59 (ddd, ^3J = 7.8 Hz, ^4J = 1.2 Hz, ^5J = 0.9 Hz, 1H, d-H), 8.25 (d, ^3J = 8.1 Hz, 1H, f-H), 7.91 (d, ^3J = 8.1 Hz, 1H, e-H), 7.87 (td, ^3J = 7.8 Hz, ^4J = 1.9 Hz, 1H, c-H), 7.60 (d, ^3J = 8.5 Hz, 2H, j-H), 7.55 (d, ^3J = 8.5 Hz, 2H, k-H), 7.33 (ddd, ^3J = 7.8 Hz, ^3J = 4.8 Hz, ^4J = 1.2 Hz, 1H, b-H), 5.50 (t, ^3J = 1.9 Hz, 2H, g-H), 4.48 (t, ^3J = 1.9 Hz, 2H, h-H), 4.15 (s, 5H, i-H), 3.22 (s, 1H, l-H). **^{13}C NMR ($CDCl_3$, 100 MHz)**: δ = 158.8, 155.8, 154.2, 149.1, 142.3, 136.8, 132.3, 131.1, 123.9, 123.7, 122.3, 121.5, 116.8, 115.6, 95.3, 90.9, 83.7, 83.2, 79.2, 69.9, 69.7, 69.6. **Elemental analysis:** Calcd for $C_{30}H_{20}FeN_2$: C, 77.60; H, 4.34; N, 6.03; found: C, 77.96; H, 4.49; N, 5.68. **ESI-MS:** Calcd for $[C_{30}H_{20}FeN_2{\cdot}H]^+$ = $[\mathbf{5}{\cdot}H]^+$, m/z = 465.1; found: $[\mathbf{5}{\cdot}H]^+$, m/z = 465.2.

5-((4-((2-Iodophenyl)ethynyl)phenyl)ethynyl)-6-ferrocenyl-2,2′-bipyridine (6). 5-((4-Ethynylphenyl)ethynyl)-6-ferrocenyl-2,2′-bipyridine (**5**, 310 mg, 668 μmol) and 1,2-iodobenzene (1.10 g, 435 μL, 3.34 mmol) were dissolved in a solution of anhydrous THF (20 mL) and anhydrous Et_3N (20 mL). The orange solution was subjected to freeze–pump–thaw procedures (3×). After addition of $Pd(PPh_3)_4$ (77.0 mg, 66.6 μmol) under N_2 atmosphere, the reaction mixture was heated at 60 °C for 18 h (followed by thin layer chromatography: TLC). The mixture was evaporated and the residue was subjected to column chromatographic purification on silica gel (ϕ = 3.5 cm, l = 30 cm) using 5% EtOAc in *n*-hexane to yield the compound **6** as an orange solid (280 mg, 420 μmol, 63%). **Mp**: 127–128 °C. **IR (KBr)**: $\tilde{\nu}$ = 3035, 2957, 2925, 2851, 2216, 1898, 1737, 1571, 1511, 1474, 1431, 1385, 1361, 1106, 1093, 1015, 1007, 826, 818, 770, 744, 737, 497 cm^{-1}. **^{1}HNMR ($CDCl_3$, 400 MHz)**: δ = 8.70 (ddd, ^3J = 4.8 Hz, ^4J = 1.8 Hz, ^5J = 0.8 Hz, 1H, a-H), 8.60 (ddd, ^3J = 7.6 Hz, ^4J = 1.0 Hz, ^5J = 0.8 Hz, 1H, d-H), 8.26 (d, ^3J = 8.1 Hz, 1H, f-H), 7.93 (d, ^3J = 8.1 Hz, 1H, e-H), 7.89 (dt, ^3J = 7.8 Hz, ^4J = 1.6 Hz, 1H, n-H), 7.87 (td, ^3J = 7.6 Hz, ^4J = 1.8 Hz, 1H, c-H), 7.66 (d, ^3J = 8.4 Hz, 2H, j-H), 7.65 (d, ^3J = 8.4 Hz, 2H, k-H), 7.56 (dd, ^3J = 7.8 Hz, ^4J = 1.6 Hz, 1H, l-H), 7.32–7.36 (m, 2H, m-, b-H), 7.04 (td, ^3J = 7.8 Hz, ^4J = 1.6 Hz, 1H, o-H), 5.52 (t, ^3J = 2.0 Hz, 2H, g-H), 4.49 (t, ^3J = 2.0 Hz, 2H, h-H), 4.13 (s, 5H, i-H). **^{13}C NMR ($CDCl_3$, 100 MHz)**: δ = 158.8, 155.8, 154.1, 149.1, 142.2, 138.8, 136.8, 132.5, 131.8, 131.2, 129.6, 129.5, 127.9, 123.9, 123.5, 123.1, 121.5, 116.8, 115.7, 101.2, 95.6, 93.7, 92.6, 91.0, 83.7, 69.9, 69.7 (2C). **Elemental analysis**: Calcd for $C_{36}H_{23}FeIN_2$: C, 64.89; H, 3.48; N, 4.20; found: C, 64.62; H, 3.41; N, 4.12. **ESI-MS**: Calcd for $[C_{36}H_{23}FeIN_2{\cdot}H]^+$ = $[\mathbf{6}{\cdot}H]^+$, m/z = 667.0; found: $[\mathbf{6}{\cdot}H]^+$, m/z = 667.1.

Nanoswitch 1. A solution of compound **7** (55.0 mg, 26.4 μmol) and 5-((4-((2-iodophenyl)ethynyl)phenyl)ethynyl)-6-ferrocenyl-2,2′-bipyridine (**6**, 53.0 mg, 79.5 μmol) in a mixture of freshly distilled anhydrous Et_3N (20 mL) and anhydrous DMF (20 mL) was degassed using freeze–pump–thaw cycles (3×). After addition of $Pd(PPh_3)_4$ (9.00 mg, 7.95 μmol), the resultant mixture was again subjected to freeze–pump–thaw cycles (2×). The reaction mixture was stirred at 60 °C for 24 h (TLC) and evaporated. The residue was dissolved in DCM (25 mL), then washed with deionized water (25 mL × 2) and a saturated brine solution (10 mL × 2). The organic phase was dried over anhydrous Na_2SO_4 and the solvent was removed. The residue was subjected to column chromatography on neutral alumina (ϕ = 3 cm, l = 20 cm) using 30% DCM in *n*-hexane (R_f = 0.30, neutral Al_2O_3, 50% DCM in *n*-hexane) to provide the crude product. The crude residue was further subjected to size-exclusion chromatography on Biobeads®-SX3 (ϕ = 2 cm, l = 55 cm) using THF as an eluent. Fractions with pure compound were combined. Compound **1** was obtained as a purple solid (15.4 mg, 5.81 μmol, 22%). **Mp**: >250 °C. **IR (KBr)**: $\tilde{\nu}$ = 3031, 2918, 2854, 2737, 2210, 1916, 1732, 1586, 1541, 1506, 1477, 1443, 1378, 1242, 1203, 1100, 1061, 996, 798, 756, 721, 542 cm^{-1}. **^{1}H NMR (CD_2Cl_2, 600 MHz)**: δ = 8.83 (d, ^3J = 4.5 Hz, 2H, β-H), 8.71 (d, ^3J = 4.5 Hz, 2H, β-H), 8.67 (dd, ^4J = 2.1 Hz, ^5J = 0.8 Hz, 1H, i-H), 8.65 (d, ^3J = 4.5 Hz, 2H, β-H), 8.63 (d, ^3J = 4.5 Hz, 2H, β-H), 8.57 (ddd, ^3J = 4.8 Hz, ^4J = 1.8 Hz, ^5J = 0.8 Hz, 1H, A-H), 8.53 (ddd, ^3J = 7.6 Hz, ^3J = 1.2 Hz, ^4J = 0.8 Hz, 1H, D-H), 8.34 (d, ^3J = 8.2 Hz, 1H, 4-H), 8.33 (d, ^3J = 8.2 Hz, 1H, 7-H), 8.23 (d, ^3J = 7.9 Hz, 2H, q-H), 8.22 (d, ^3J = 8.1 Hz, 1H, E-H), 8.18 (t, ^3J = 7.7 Hz, 1H, e-H), 8.13 (d, ^3J = 8.2 Hz, 1H, g-H), 7.93 (d, ^3J = 7.9 Hz, 2H, p-H), 7.92 (d, ^3J = 8.1 Hz, 1H, F-H), 7.90 (2 s, merged, 2H, 5-, 6-H), 7.89 (dd, ^3J = 8.2 Hz, ^4J = 2.1 Hz, 1H, h-H), 7.74 (td, ^3J = 7.6 Hz, ^4J = 1.8 Hz, 1H, C-H), 7.68 (d, ^3J = 8.5 Hz, 2H, j/k-H), 7.67 (2 d, merged, ^3J = 8.2 Hz, 4H, J-, K-H), 7.57–7.63 (m, 16H, d-, f-, l-, o-, L-, O-, tpc-H), 7.56 (d, ^3J = 8.2 Hz, 1H, 3-H), 7.53 (d, ^3J = 8.2 Hz, 1H, 8-H), 7.34–7.44 (m, 12H, k/j-, m-, n-, M-, N-, tpc-H), 7.33 (s, 2H, s-H), 7.24 (s, 4H, r-H), 7.20 (ddd, ^3J = 7.6 Hz, ^3J = 4.8 Hz, ^4J = 1.2 Hz, 1H, B-H), 6.95 (s, 2H, z-H), 6.83 (d, ^3J = 5.8 Hz, 1H, c-H), 5.49 (t, ^3J = 1.8 Hz, 2H, G-H), 4.48 (t, ^3J = 1.8 Hz, 2H, H-H), 4.10 (s, 5H, I-H), 3.76 (s, 1H, a-H), 2.73 (d, ^3J = 5.8 Hz, 1H, b-H), 2.64 (s, 3H, w-H), 2.58 (s, 6H, u-H), 2.52 (s, 6H, 9-H), 2.32 (s, 3H, y-H), 2.04 (s, 6H, x-H), 1.94 (s, 6H, v-H), 1.93 (s, 6H, 10-H), 1.74 (s, 12H, t-H). **^{13}C NMR (CD_2Cl_2, 100 MHz)**: δ = 162.6, 161.4, 160.5, 159.2, 156.0, 155.0, 154.6, 154.3, 152.9, 151.5, 151.4, 151.2 (2C), 150.2 (2C), 149.9, 149.7, 149.4, 146.9, 146.8, 146.6, 146.5, 146.1, 144.1, 142.6, 141.9, 140.3, 139.8 (2C), 139.6, 139.5, 138.5, 138.2, 137.8, 137.7, 137.6, 137.0, 136.6, 136.4 (2C), 136.1, 135.1, 132.6 (2C), 132.4, 132.3, 132.2 (2C), 132.1, 132.0, 131.7, 131.6 (3C), 131.5 (2C), 131.3 (3C), 131.2, 130.9, 130.1, 128.8 (2C), 128.6 (2C), 127.9, 127.8, 127.6 (2C), 126.6, 126.5, 126.1, 125.7, 125.4, 124.9, 124.8, 124.1 (2C), 123.8 (2C), 123.1, 123.0, 122.9, 122.6, 122.3, 121.8, 121.6 (2C), 121.5, 121.3, 120.7, 118.9 (3C), 118.8, 117.1, 116.0, 96.8, 95.9, 93.9, 93.8, 93.6, 93.5, 93.3, 91.4, 90.8, 90.7, 90.3, 90.1, 89.8, 88.9, 88.8, 88.6, 84.1, 70.3, 70.1, 65.5, 22.0, 21.8, 21.6, 21.5, 21.2, 20.4, 18.6, 17.7. **Elemental analysis**: Calcd for $C_{183}H_{130}FeN_{12}Zn{\cdot}CH_2Cl_2{\cdot}MeOH$: C, 81.23; H, 5.01; N, 6.14; found: C, 81.07; H, 5.40; N, 5.81. **ESI-MS**: Calcd for $[C_{183}H_{130}FeN_{12}Zn{\cdot}2H]^{2+}$ = $[\mathbf{1}{\cdot}2H]^{2+}$, m/z = 1309.5; $[C_{183}H_{130}FeN_{12}Zn{\cdot}3H]^{3+}$ = $[\mathbf{1}{\cdot}3H]^{3+}$, m/z = 873.3; found: $[\mathbf{1}{\cdot}2H]^{2+}$, m/z = 1309.7; $[\mathbf{1}{\cdot}3H]^{3+}$, m/z = 873.5.

Complex $[Cu(1)]^+$. CD_2Cl_2 was added to a mixture of $[Cu(CH_3CN)_4]{\cdot}B(C_6F_5)_4$ (324 μg, 0.357 μmol) and nanoswitch **1** (935 μg, 0.357 μmol) in an NMR tube. The reddish purple solution was submitted for NMR without further purification. **Yield**: 96% (by NMR). Signals attest the occurrence of two diastereomers in 55 : 45 ratio (due to the stereogenic center and axis). **IR (KBr)**: $\tilde{\nu}$ = 3034, 2955, 2916, 2856, 2210, 1916, 1720, 1641, 1582, 1549, 1510, 1461, 1389, 1273, 1203, 1086, 979, 821, 800, 774, 755, 683 cm^{-1}. **^{1}H NMR (CD_2Cl_2, 600 MHz)**: δ = 8.86 (d, ^3J = 4.5 Hz, 1H, β-H), 8.84 (d, ^3J = 4.5 Hz, 1H, β-H), 8.72 (2 d, ^3J = 4.6 Hz, 2H, β-H), 8.68–8.70 (m, 2H, 7/4-, i-H), 8.67 (3 d, ^3J = 4.5 Hz, 3H, β-H), 8.64 (d, ^3J = 4.5 Hz, 1H, β-H), 8.55 (d, ^3J = 8.2 Hz, 1H, 4/7-H), 8.29 (d, ^3J = 8.2 Hz, 1.1H, q-H), 8.27 (d, ^3J = 8.2 Hz, 0.9H, q-H), 8.13–8.22 (m, 5H, D-, 5-, 6-, e-, g-H), 8.09 (d, ^3J = 8.4 Hz, 0.45H, F-H), 8.08 (d, ^3J = 8.4 Hz, 0.55H, F-H), 8.01 (dd, ^3J = 8.2 Hz, ^4J = 2.1 Hz, 1H, h-H), 7.98 (d, ^3J = 8.2 Hz, 0.9H, p-H), 7.95 (d, ^3J = 8.2 Hz, 1.1H, p-H), 7.92 (td, ^3J = 7.6 Hz, ^4J = 1.6 Hz, 1H, C-H), 7.85 (d, ^3J = 8.2 Hz, 0.55H, 3/8-H), 7.84 (d, ^3J = 8.4 Hz, 0.45H, 3/8-H), 7.76–7.78 (m, 1H, E-H), 7.71 (d, ^3J = 8.4 Hz, 1H, tpc-H), 7.56–7.68 (m, 20H, A-, d-, f-, l-, o-, L-, O-, 8/3-, j/k-, J/K-, tpc-H), 7.53 (d, ^3J = 8.4 Hz, 1H, tpc-H), 7.40–7.50 (m, 6H, tpc-H), 7.36–7.38 (m, 4H, k/j-, K/J-H), 7.331 (s, 1.1H, s-H), 7.327 (s, 0.9H, s-H), 7.26–7.32 (m, 4H, M-, N-, m-, n-H), 7.25 (s, 2.2H, r-H), 7.24 (s, 1.8H, r-H), 7.18–7.22 (m, 1H, B-H), 6.97 (s, 0.55 H, z-H), 6.96 (s, 0.45 H, z-H), 6.860 (d, ^3J = 5.8 Hz, 0.55H, c-H), 6.858 (d, ^3J = 5.8 Hz, 0.45H, c-H), 6.72 (s, 0.55 H, z-H), 6.70 (s, 0.45 H, z-H), 5.76–5.78 (m, 2H, G-H), 4.49–4.51 (m, 2H, H-H), 4.01 (s, 2.75 H, I-H), 3.99 (s, 2.25 H, I-H), 3.80 (s, 0.55H, a-H), 3.78 (s, 0.45H, a-H), 2.75 (d, ^3J = 5.8 Hz, 0.45H, b-H), 2.74 (d, ^3J = 5.8 Hz, 0.55H, b-H), 2.644 (s, 1.65H, w-H), 2.641 (s, 1.35H, w-H), 2.60 (s, 3.3H, u-H), 2.58 (s, 2.7H, u-H), 2.46 (s, 3H, 10-H), 2.24 (s, 1.65H, x-H), 2.22 (s, 1.35H, x-H), 2.13 (s, 1.65H, x-H), 2.12 (s, 1.35H, x-H), 1.95 (s, 3.3H, v-H), 1.94 (s, 2.7H, v-H), 1.89 (s, 3H, 10-H), 1.75 (s, 3.3H, t-H)*, 1.74 (s, 6H, t-H), 1.73 (s, 2.7H, t-H)*, 1.57 (s, 1.65H, y-H), 1.55 (s, 1.35H, y-H), 1.28 (s, 1.65H, 9-H), 1.27 (s, 1.35H, 9-H), 0.82 (s, 1.65H, 9-H), 0.81 (s, 1.35H, 9-H). **Elemental analysis**: Calcd for $C_{207}H_{130}BCuF_{20}FeN_{12}Zn{\cdot}2.5CH_2Cl_2$: C, 70.42; H, 3.81; N, 4.70; found: C, 70.45; H, 3.48; N, 4.61. **ESI-MS**: Calcd for $[C_{183}CuH_{130}FeN_{12}Zn{\cdot}MeCN{\cdot}H_2O]^{2+}$ = $[Cu(\mathbf{1}){\cdot}MeCN{\cdot}H_2O]^+$, m/z = 2740.9; found: $[Cu(\mathbf{1}){\cdot}MeCN{\cdot}H_2O]^+$, m/z = 2741.1.

*The distinct shifts of t-H indicate a different angle at the N_{azatpy} → ZnPor unit as a result of diastereomer formation.

Conflicts of interest

There are not conflicts to declare.

Acknowledgements

We are grateful to the DAAD (Deutscher Akademischer Austauschdienst), DFG (Deutsche Forschungsgemeinschaft, Schm-647/19-2), and the Universität Siegen for financial support. We thank Abir Goswami for determination of a binding constant.

References

1 Selected reviews: (*a*) M. Nishikawa, S. Kume and H. Nishihara, *Phys. Chem. Chem. Phys.*, 2013, **15**, 10549–10565; (*b*) S. Erbas-Cakmak, D. A. Leigh, C. T. McTernan and A. L. Nussbaumer, *Chem. Rev.*, 2015, **115**, 10081–10206; (*c*) A. J. McConnell, C. S. Wood, P. P. Neelakandan and J. R. Nitschke, *Chem. Rev.*, 2015, **115**, 7729; (*d*) N. Le Poul and B. Colasson, *ChemElectroChem*, 2015, **2**, 475–496; (*e*) S. Ø. Scottwell and J. D. Crowley, *Chem. Commun.*, 2016, **52**, 2451–2464; (*f*) Y. Wang, M. Frasconi and J. F. Stoddart, *ACS Cent. Sci.*, 2017, **3**, 927–935; (*g*) T. Fukino, H. Yamagishi and T. Aida, *Adv. Mater.*, 2017, **29**, 1603888; (*h*) A. Goswami and M. Schmittel, *Coord. Chem. Rev.*, 2018, **376**, 478–505.

2 (*a*) F. Niess, V. Duplan and J.-P. Sauvage, *J. Am. Chem. Soc.*, 2014, **136**, 5876–5879; (*b*) S. K. Samanta, A. Rana and M. Schmittel, *Dalton Trans.*, 2014, **43**, 9438–9447; (*c*) J. Sun, Y. Wu, Y. Wang, Z. Liu, C. Cheng, K. J. Hartlieb, M. R. Wasielewski and J. F. Stoddart, *J. Am. Chem. Soc.*, 2015, **137**, 13484–13487; (*d*) M. Schmittel, S. De and S. Pramanik, *Org. Biomol. Chem.*, 2015, **13**, 8937–8944; (*e*) S. Ø. Scottwell, A. B. S. Elliott, K. J. Shaffer, A. Nafady, C. J. McAdam, K. C. Gordon and J. D. Crowley, *Chem. Commun.*, 2015, **51**, 8161–8164; (*f*) C. R. Benson, A. I. Share, M. G. Marzo and A. H. Flood, *Inorg. Chem.*, 2016, **55**, 3767–3776; (*g*) H. V. Schröder, S. Sobottka, M. Nößler, H. Hupatz, M. Gaedke, B. Sarkar and C. A. Schalley, *Chem. Sci.*, 2017, **8**, 6300–6306; (*h*) C. Pezzato, M. T. Nguyen, C. Cheng, D. J. Kim, M. T. Otley and J. F. Stoddart, *Tetrahedron*, 2017, **73**, 4849–4857; (*i*) Y. Wang, J. Sun, Z. Liu, M. S. Nassar, Y. Y. Botros and J. F. Stoddart, *Chem. Sci.*, 2017, **8**, 2562–2568; (*j*) S. Gaikwad, S. Pramanik, S. De and M. Schmittel, *Dalton Trans.*, 2018, **47**, 1786–1789; (*k*) D. T. Payne, W. A. Webre, Y. Matsushita, N. Zhu, Z. Futera, J. Labuta, W. Jevasuwan, N. Fukata, J. S. Fossey, F. D'Souza, K. Ariga, W. Schmitt and J. P. Hill, *Nat. Commun.*, 2019, **10**, 1007.

3 (*a*) B. S. L. Collins, J. C. M. Kistemaker, E. Otten and B. L. Feringa, *Nat. Chem.*, 2016, **8**, 860–866; (*b*) B. Doistau, L. Benda, J.-L. Cantin, L.-M. Chamoreau, E. Ruiz, V. Marvaud, B. Hasenknopf and G. Vives, *J. Am. Chem. Soc.*, 2017, **139**, 9213–9220.

4 (*a*) H. Zhang, X.-X. Kou, Q. Zhang, D.-H. Qu and H. Tian, *Org. Biomol. Chem.*, 2011, **9**, 4051–4056; (*b*) F. Durola, V. Heitz, F. Reviriego, C. Roche, J.-P. Sauvage, A. Sour and Y. Trolez, *Acc. Chem. Res.*, 2014, **47**, 633–645; (*c*) S. Gaikwad, A. Goswami, S. De and M. Schmittel, *Angew. Chem., Int. Ed.*, 2016, **55**, 10512–10517; (*d*) I. Aprahamian, *Chem. Commun.*, 2017, **53**, 6674–6684; (*e*) M. Baroncini, M. Canton, L. Casimiro, S. Corra, J. Groppi, M. La Rosa, S. Silvi and A. Credi, *Eur. J. Inorg. Chem.*, 2018, 4589–4603; (*f*) B. Mondal, A. Kumar Ghosh and P. S. Mukherjee, *J. Org. Chem.*, 2017, **82**, 7783–7790; (*g*) C. Burkhart and G. Haberhauer, *Eur. J. Org. Chem.*, 2017, 1308–1317; (*h*) S. Kassem, T. van Leeuwen, A. S. Lubbe, M. R. Wilson, B. L. Feringa and D. A. Leigh, *Chem. Soc. Rev.*, 2017, **46**, 2592–2621; (*i*) S. Gaikwad and M. Schmittel, *J. Org. Chem.*, 2017, **82**, 343–352; (*j*) H. V. Schröder, J. M. Wollschläger and C. A. Schalley, *Chem. Commun.*, 2017, **53**, 9218–9221.

5 W. Jiang and C. A. Schalley, *Proc. Natl. Acad. Sci. U. S. A.*, 2009, **106**, 10425–10429.

6 (*a*) S. Pramanik, S. De and M. Schmittel, *Angew. Chem., Int. Ed.*, 2014, **53**, 4709–4713; (*b*) S. Pramanik, S. De and M. Schmittel, *Chem. Commun.*, 2014, **50**, 13254–13257.

7 M. L. Saha, S. Neogi and M. Schmittel, *Dalton Trans.*, 2014, **43**, 3815–3834.

8 M. Schmittel, V. Kalsani, P. Mal and J. W. Bats, *Inorg. Chem.*, 2006, **45**, 6370–6377.

9 M. Schmittel, S. De and S. Pramanik, *Angew. Chem., Int. Ed.*, 2012, **51**, 3832–3836.

10 F. L. Hedbern and H. Rosenberg, *Tetrahedron Lett.*, 1969, **10**, 4011–4012.

11 A. G. Bonn and O. S. Wenger, *J. Org. Chem.*, 2015, **80**, 4097–4107.

12 M. Schmittel, S. Pramanik and S. De, *Chem. Commun.*, 2012, **48**, 11730–11732.

13 F. A. Bell, A. Ledwith and D. C. Sherrington, *J. Chem. Soc. C*, 1969, 2719–2720.

14 (*a*) R. Breuer and M. Schmittel, *Organometallics*, 2012, **31**, 6642–6651; (*b*) R. Breuer and M. Schmittel, *Organometallics*, 2013, **32**, 5980–5987.